Jet Flowfield behind a Laser-Supported Detonation Wave

P. D. Thomas*
Lockheed Palo Alto Research Laboratories, Palo Alto, Calif.

The axisymmetric flowfield behind a strong laser-supported detonation (LSD) wave is studied theoretically. The LSD-induced flowfield is steady in wave-fixed coordinates, and is analogous to that created by a sonic rocket nozzle exhausting into a coflowing hypersonic freestream. A characteristic feature of such flows is a strong axial jet of exhaust gas that persists for hundreds of nozzle diameters downstream. The LSD-induced flow is shown to obey the hypersonic similarity principle, and to scale in a simple fashion as a function of the parameters that characterize the laser beam. This implies the existence of a universal solution that is valid for any LSD wave supported by a uniform cylindrical beam and steady laser flux. The solution, obtained numerically, exhibits a strong axial jet of laser-heated plasma flowing in the same direction as the incident laser radiation, whereas the LSD wave propagates in the opposite direction. A comparison reveals deficiencies in the cylindrical blast-wave model that has been used widely to estimate the conditions far behind the LSD wave. The model is found to yield reasonable asymptotic estimates of the pressure and radial velocity fields and of the outer shock radius. However, the model fails to predict the cooling rate of the laser-heated plasma. An alternative asymptotic model is developed that provides reliable analytic estimates of the flowfield parameters.

I. Introduction

STRONG laser-supported detonation (LSD) waves in air are easily generated experimentally by irradiating opaque metal targets with laser beams of sufficiently high intensity[1]. These waves propagate away from the target at hypersonic speed in the direction opposite to the laser radiation flux. The LSD wave front itself has been successfully modeled by Raizer[2] as a thin, shock-like region within which virtually all the incident laser energy is absorbed and the air is heated to high temperatures and pressures. This creates a complicated flowfield of hot plasma interacting both with the ambient air and with the target. The prediction of the heat transfer, pressure, and impulse transmitted to the target requires rather detailed knowledge of the flowfield set up by the LSD wave, and how this flowfield scales as a function of the laser flux and laser-beam diameter. The theoretical analysis presented below provides a quantitative description of this flowfield for an LSD wave propagating freely in air in the absence of the target. The LSD wave is assumed to be supported by a steady, uniform, cylindrical laser beam. The analysis would be expected to apply in the case of an LSD wave generated at the surface of a target once the wave has traveled a distance of several beam diameters from the surface.

II. Formulation

We shall analyze in detail the axisymmetric flowfield behind a strong LSD wave supported in air by a laser beam of diameter d and steady flux f that is spatially uniform over the beam area. According to Raizer's theory,[2] the wave moves toward the laser energy source with the absolute velocity

$$V=[2(\gamma^2-1)f/\rho_o]^{1/3} \tag{1}$$

where ρ_o is the density of the air ahead of the wave and $\gamma \approx 1.2$ is the effective specific heat ratio of the hot air behind the LSD wave. This velocity is always hypersonic.[2] The entire flowfield is steady when viewed in terms of a coordinate system fixed on the LSD wave (Fig. 1). The laser-heated plasma emerges from the wave at locally sonic conditions[2] and its pressure is large compared to that of the ambient air. Thus, the flowfield behind the wave is identical to that set up by a highly underexpanded rocket exhaust issuing from a sonic nozzle into a hypersonic freestream traveling in the same direction as the exhaust. The qualitative structure of this type of flow is well understood.[3,4] As shown in Fig. 1 the interaction of the two streams produces an adiabatic shock wave in the freestream. The exhaust gas expands and accelerates in the axial direction and becomes a strong, high-speed jet that persists for many hundreds of nozzle diameters downstream. The initial pressure mismatch between the two streams usually causes an overexpansion of the exhaust gas, which then is recompressed through an embedded shockwave that propagates inward toward the axis of symmetry. If the freestream Mach number is low, the embedded shock undergoes a Mach reflection at the axis, although a regular reflection is thought to occur for high freestream Mach numbers.[3] The flowfield is predominantly inviscid for an appreciable distance downstream, with viscous effects confined to a thin shear layer at the outer edge of the exhaust gas jet.

We shall confine our attention to the inviscid part of the LSD wave-induced flowfield, which is governed by the following equations in the axisymmetric cylindrical coordinates (z,r)

$$(\rho u)_z+(1/r)(r\rho v)_r=0 \tag{1a}$$

$$(\rho uv)_z+p_r+(1/r)(r\rho v^2)_r=0 \tag{1b}$$

$$(p+\rho u^2)_z+(1/r)(r\rho uv)_r=0 \tag{1c}$$

$$(\rho uH)_z+(1/r)(r\rho vH)_r=0 \tag{1d}$$

The subscripts denote partial derivatives; ρ is the density; p the pressure; u and v the axial and radial velocity components, respectively; and H the specific total enthalpy

$$H=h+(u^2+v^2)/2 \tag{2}$$

with h the specific static enthalpy. These equations are written in dimensionless form, with all distances normalized by the laser beam diameter d, velocities normalized by the LSD wave velocity V, enthalpies normalized by V^2, density normalized by the freestream density ρ_0 and pressure normalized by the freestream momentum flux $\rho_0 V^2$. The system of equations is

Presented as Paper 77-28 at the AIAA 15th Aerospace Sciences Meeting, Los Angeles, Calif., Jan. 24-26, 1977; submitted Jan. 24, 1977; revision received June 15, 1977.

Index categories: Lasers; Shock Waves and Detonations; Jets, Wakes, and Viscid-Inviscid Flow Interactions.

*Staff Scientist. Member AIAA.

closed by the perfect gas relations

$$p=(\gamma-1)\rho h/\gamma$$

$$c=\sqrt{\gamma p/\rho}$$

where c is the sound speed.

We position the origin $z=0$ of the coordinate system at the LSD wave. The initial values of the dimensionless flow variables immediately behind the LSD wave are[2]

$$p=1/(\gamma+1) \qquad \rho=(\gamma+1)/\gamma$$

$$h=\gamma^2/(\gamma+1)^2(\gamma-1) \qquad u=c=\gamma/(\gamma+1)$$

$$v=0 \qquad \text{for } z=0,\ 0\le r\le \tfrac{1}{2} \tag{3}$$

The symmetry boundary conditions that apply along the axis of symmetry are

$$v=u_r=p_r=\rho_r=0 \text{ at } r=0 \tag{4}$$

Because the LSD wave velocity is always hypersonic, we may employ the strong shock approximation along the outer adiabatic shock wave $r=s(z)$ that extends into the freestream beyond the laser beam radius $r>\frac{1}{2}$. The flow variables immediately behind the shock then depend only on the local inclination angle θ between the shock and the symmetry axis through the equations

$$p_s=[2/(\gamma+1)]\sin^2\theta \tag{5a}$$

$$\rho_s=(\gamma+1)/(\gamma-1) \tag{5b}$$

$$u_s=1-[2/(\gamma+1)]\sin^2\theta \tag{5c}$$

$$v_s=[2/(\gamma+1)]\sin\theta\cos\theta \tag{5d}$$

The equations and boundary conditions (1-5) govern the jet flowfield downstream of the LSD wave. As expressed in their nondimensional form, neither the equations nor the boundary conditions contain any explicit dependence on the laser beam diameter and laser flux f that drives the LSD wave. This behavior is in keeping with the hypersonic similarity principle,[5] and is valid throughout the regime where the outer adiabatic shockwave is strong in the sense that the density jump across the shock is constant. Thus, Eqs. (1-5) yield a universal solution that applies to any strong LSD wave through the scaling implied by the definitions of the nondimensional variables, regardless of the laser beam parameters d and f or of the external air density ρ_0.

III. Method of Solution

The universal solution has been obtained numerically with the aid of a finite-difference computer code. Most of the basic numerical methods employed in the code have been described by Thomas et al.,[6] as applied to three-dimensional, supersonic, isoenergetic flows ($H=$const) that involve no embedded shockwaves. In the present application, the total enthalpy of the laser-heated plasma inside the contact surface differs from that in the shocked air layer, and it is necessary to solve the energy equation (1d) as well as the continuity and momentum equations (1a-c). The equations are expressed in conservation-law form to enable the code to compute embedded shockwaves and contact discontinuities as smeared transitions. However, the outer shockwave is treated as a sharp discontinuity using the technique described by Thomas et al.[6]

The boundary conditions at the axis of symmetry are computed using a variant of Kentzer's scheme.[14] The pressure is computed from a finite-difference representation of a characteristic compatibility relation. The axial mass flow ρu and the total enthalpy H computed from Eqs. (1a) and (1d), together with the equation of state and the boundary condition $v=0$, then suffice to determine all the flow variables at the axis.

The code computes the entire flowfield between the axis and the outer shockwave by forward integration in the axial (z) direction, starting from an initial data line normal to the axis and located just downstream of the LSD wave. This is permissible as long as the axial velocity component is everywhere supersonic.

$$u>c \tag{6}$$

for then the governing equations (1) are z hyperbolic and z is a time-like coordinate. The integration is performed using MacCormack's second-order finite-difference scheme.[7]

There are two difficulties that must be overcome in order to start the numerical solution: 1) the flow is sonic just downstream of the LSD wave, whereas the numerical algorithm requires $u>c$, and 2) a singularity exists at the edge of the LSD wave. The first difficulty is avoided simply by using an initial Mach number slightly above unity in the region $0\le r<\frac{1}{2}$. Love et al.[4] previously encountered the same difficulty in attempting to start method-of-characteristics solutions for sonic jets. They found that an initial value of Mach 1.01 gave good results, and we have employed this value successfully. The appropriate initial conditions are obtained from Eqs. (3) by applying a weak isentropic expansion that accelerates the flow from Mach 1 to Mach 1.01.

The second difficulty requires a more extensive analysis. It is easily demonstrated that the point $(z,r)=(0,\frac{1}{2})$ at the edge of the LSD wave is a singularity of the flow equations (1) under the boundary conditions (3) and (5). Howe[8] was the first to investigate the nature of the singularity and to construct a local solution. The qualitative character of the solution is illustrated in Fig. 1. An adiabatic oblique shockwave and a contact surface, both of which are locally straight, emanate from the singular point. The laser-heated plasma emerging from the LSD wave undergoes a Prandtl-Meyer expansion, and the contact surface and shock inclination angles are uniquely determined by the requirement that the pressure be continuous across the contact surface. This local solution is valid provided that the contact surface angle

$$\delta=\tan^{-1}(v_s/u_s)$$

does not exceed the limiting value above which the oblique shock becomes detached[9]

$$\delta<\sin^{-1}(1/\gamma)$$

The equivalent bound on the shock pressure is, for a strong shock,

$$p_s<1/\gamma \tag{7}$$

for attachment. The continuity of pressure at the contact surface demands that

$$p_s=p_c \tag{8}$$

where p_c is the pressure of the laser-heated gas just inside the contact surface. The latter cannot exceed the initial pressure prior to expansion as given by Eqs. (3). Thus, we find that the shock pressure has the upper bound

$$p_s\le 1/(\gamma+1)$$

The latter is well below the attachment limit as given by Eq. (7), so that Howe's solution is valid in the strong shock regime.

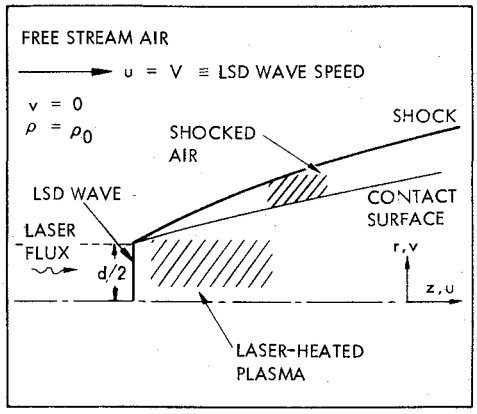

Fig. 1 Sketch of LSD-induced flowfield.

To find the contact surface angle and pressure, we employ the following relation between the flow deflection angle and the pressure behind the oblique shock[9]

$$\tan\delta = v_s/u_s = \left\{p_s\left[\frac{2}{\gamma+1} - p_s\right]\right\}^{1/2}/(1-p_s) \tag{9}$$

along with the Prandtl-Meyer relation[9] between the pressure and turning angle of the laser-heated plasma just inside the contact surface

$$\delta = A^{1/2}\tan^{-1}B^{1/2} - \tan^{-1}(AB)^{1/2}$$

$$A = (\gamma+1)/(\gamma-1)$$

$$B = [(\gamma+1)p_c]^{(1-\gamma)/\gamma} - 1 \tag{10}$$

For $\gamma = 1.2$ the solution to Eqs. (8-10) is

$$\delta = 22.5 \text{ deg}, \quad p_s = p_c = 0.162 \tag{11}$$

From Eq. (5a), the corresponding shock angle is $\theta = 25.0$ deg. The remaining flow variables between the shock and contact surface can be found from the shock relations (5), and the flow variables in the plasma just inside the contact surface can be computed from the pressure p_c with the aid of the well-known isentropic flow relations that apply along streamlines passing through the Prandtl-Meyer expansion fan.

IV. Numerical Results

A numerical solution for the flowfield up to 100 laser beam diameters downstream of the LSD wave has been obtained using a radial grid of 50 mesh intervals evenly distributed between the symmetry axis and the outer air shock. Selected numerical results are displayed in Figs. 2-8 for a specific heat ratio $\gamma = 1.2$ both in the laser-heated plasma and in the shock-heated air region. Figure 2 shows the initial shockwave trajectory, drawn to scale, along with the approximate trajectory of the contact surface as computed by tracing the streamline emanating from the singular point at the edge of the LSD wave. Also shown is the trajectory of a weak embedded shock that originates in the laser-heated plasma core near the contact surface, and that undergoes multiple reflections at the axis and at the contact surface. The peak pressure ratio across this embedded shock never exceeds about 3.0. The shock is apparently too weak to experience Mach reflection at the axis, although one cannot discount the possibility that the real flowfield might contain a Mach disk that is simply too small in lateral dimension to be resolved by the finite-difference grid.† The embedded shock gradually weakens and is no longer readily discernible in the computation beyond its second reflection at the axis.

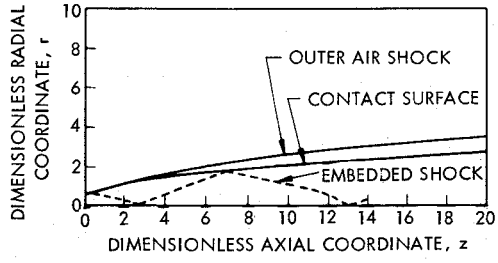

Fig. 2 Computed flowfield geometry.

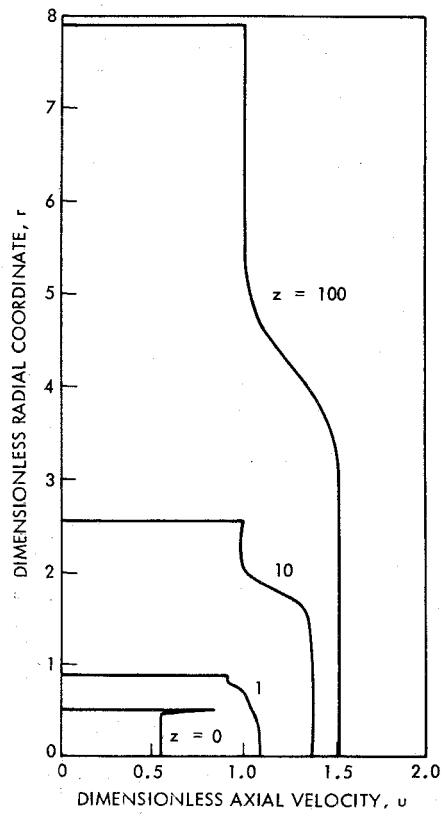

Fig. 3 Axial velocity profiles.

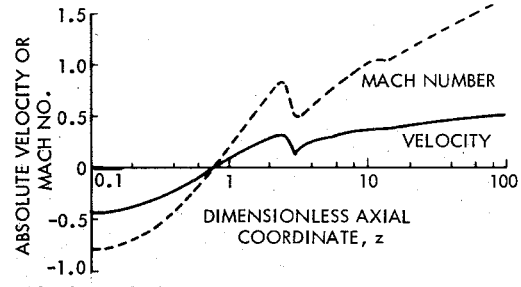

Fig. 4 Absolute velocity $(u-1)$ and Mach number $(u-1)/c$ along jet axis.

The axial velocity profiles of Fig. 3 show clearly the development of a strong jet in the laser-heated plasma. In the region beyond approximately one laser beam diameter downstream of the LSD wave itself, the velocity in the jet actually exceeds the LSD wave speed. This means that a fixed observer would see a jet of hot plasma moving in the same direction as the laser radiation flux, whereas the LSD wave propagates in the opposite direction. This is demonstrated clearly by plotting the dimensionless absolute particle velocity $u-1$ along the jet centerline (Fig. 4). Within the first beam

†The numerical scheme is incapable of actually computing the flow through a Mach disk, behind which the inequality (6) is violated.

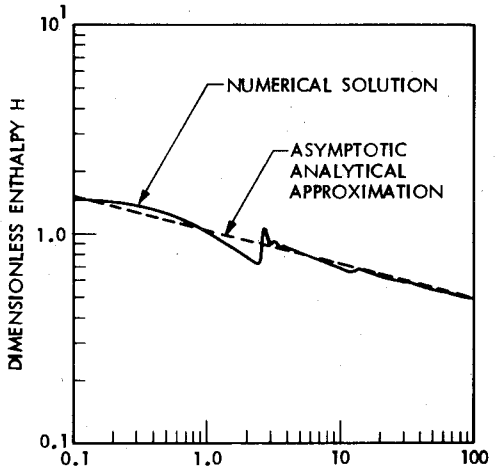

Fig. 5 Static enthalpy distribution along axis.

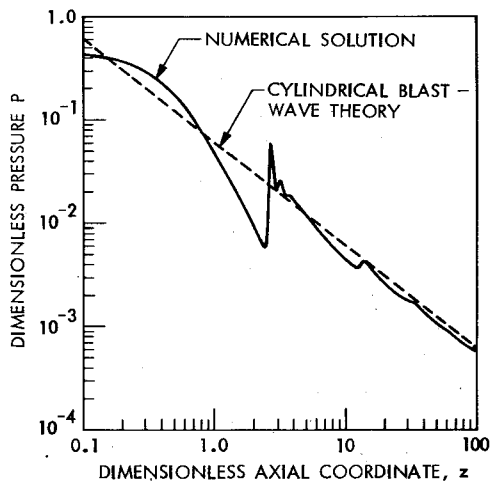

Fig. 6 Pressure distribution along axis.

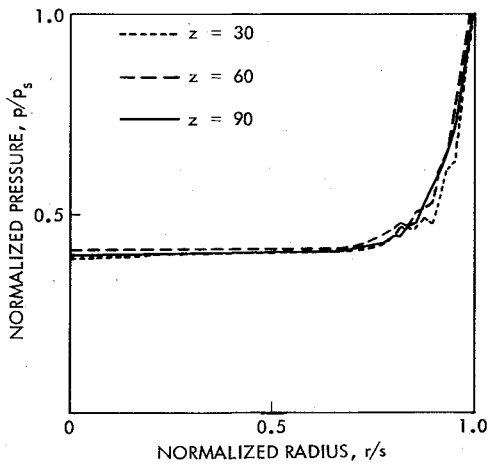

Fig. 7 Pressure profiles.

diameter aft of the LSD wave; the flow moves with the wave ($u-1<0$). Farther back, however, the flow is directed away from the wave ($u-1>0$). Figure 4 also shows the absolute Mach number along the centerline. The Mach number remains fairly low so that the stagnation pressure and temperature are roughly of the same order of magnitude as the static values. The jet cools rather slowly with distance from the LSD wave, although the pressure decays rapidly (Figs. 5 and 6).

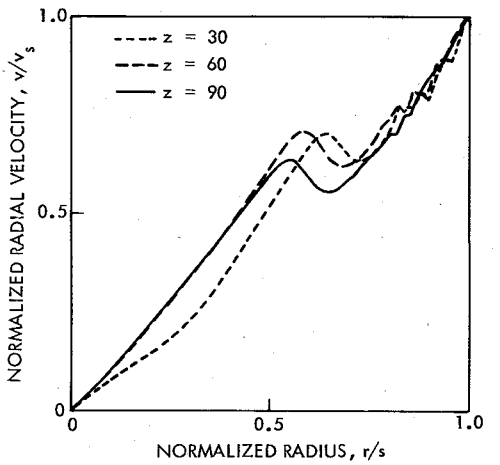

Fig. 8 Radial velocity profiles.

Sufficiently far from the LSD wave, the radial pressure profiles plotted in Fig. 7 display an approximately self-similar behavior, and closely resemble the pressure profile in an unsteady cylindrical blast wave.[10] The radial velocity profiles shown in Fig. 8 also exhibit self-similarity except in the immediate neighborhood of the contact surface, across which jumps occur in both velocity components (cf. Fig. 3).

V. Comparison with Cylindrical Blast-Wave Theory

A number of investigators have employed a model based upon cylindrical blast-wave theory to estimate the pressure and impulse imparted to a fixed target located at beam diameter or more behind an LSD wave.[11-13] According to this model the pressure on a surface located at a physical distance $z' \gg d$ behind the LSD wave is analogous to the pressure within a cylindrical blast wave at time‡ $t'=z'/V$ after detonation of a line charge whose energy per unit length E_0 is the same as that deposited in the LSD wave by the incident laser beam

$$E_0 = \pi d^2 f/4V \tag{12}$$

Similarly, the radius of the outer air shock $r'=s'(z')$ behind the LSD wave is analogous to the radius of the cylindrical blast wave at time t'.

We observe that the analogy is inexact because it fails to account for axial motion of the gas. Nevertheless, it is useful to compare the predictions of the model with our numerical solution to the exact equations of motion because the model has been widely used.

The self-similar solution for the blast-wave radius and pressure, and the pressure level and radial velocity gradient near the center of symmetry are[10]

$$s' = (E_0/\alpha\rho_0)^{1/4}(t')^{1/2} \tag{13a}$$

$$p_s' = [\rho_0/2(\gamma+1)](E_0/\alpha\rho_0)^{1/2}(t')^{-1} \tag{13b}$$

$$p' = \beta p'_s \tag{13c}$$

$$\frac{\partial v'}{\partial r'} = (2\gamma t')^{-1} \tag{13d}$$

where the proportionality constants α,β depend only on γ, and have the values

$$\alpha \approx 2,\ \beta \approx 0.426 \text{ for } \gamma = 1.2 \tag{13e}$$

‡The superscript prime is used where needed to distinguish physical dimensional variables from dimensionless (unprimed) variables.

We note that $\partial v'/\partial r'$ is very nearly constant between the center of symmetry and the blast wave. This is also true of the pressure p' except for a narrow layer in the immediate neighborhood of the blast wave.

In terms of the dimensionless variables introduced earlier, the blast-wave predictions (13) for the flow variables behind the LSD wave with $\gamma = 1.2$ are

$$\left.\begin{aligned} s &= 0.817z^{1/2} \\ p_s &= 0.152z^{-1} \\ p &= 0.0647z^{-1} \\ \frac{\partial v}{\partial r} &= (2\gamma z)^{-1} \end{aligned}\right\} \quad \text{near } r=0 \tag{14}$$

The logarithmic plot of the computed shockwave trajectory in Fig. 9 reveals that Eq. (14a) accurately predicts the asymptotic behavior for $z \gg 1$. The blast-wave model also provides a fairly good approximation to the asymptotic behavior of the pressure along the axis of the jet, as shown in Fig. 6. The radial velocity gradient within the jet core $r < r_c$ also is predicted reasonably well by Eq. (14d).

The described comparisons explain why the blast-wave model has enjoyed some success in predicting the pressure and impulse imparted to a target in cases where the laser pulse duration is sufficiently long to allow the asymptotic regime to be realized.[11-13] However, other major characteristics of the LSD jet flowfield are incorrectly represented by the model. This is particularly true of those characteristics such as axial velocity and enthalpy that affect the heat transfer to a surface. For example, the blast-wave solution predicts that the density vanishes and the enthalpy is unbounded near the center of symmetry $r = 0$, whereas the exact numerical solution behaves differently. Moreover, the blast-wave model implies that the density profile ρ/ρ_s vs r/s is invariant with z, so that the enthalpy $h \sim p/\rho \sim z^{-1}$, since ρ_s is constant in the strong shock regime. This cooling rate is much faster than that evinced by the numerical solution (Fig. 5). The numerical solution displays a more gradual cooling rate such that the enthalpy in the laser-heated jet decays approximately as $h \sim z^{-(\gamma-1)/\gamma}$ We shall present an alternative model that, unlike the blast-wave model, agrees in all respects with the numerical solution.

VI. Approximate Model of the Jet Flowfield

We have seen that Eqs. (14), based upon the blast-wave model, adequately represent the pressure, radial velocity field, and outer shock radius in the asymptotic region $z \gg 1$. The model is grossly in error in all other respects. However, very simple methods can be employed to obtain valid estimates of the density, enthalpy, and axial velocity in the jet, and of the contact surface radius r_c. The numerical solution shows that the flow of laser-heated plasma inside the contact surface is very nearly isentropic because the embedded shocks are weak. Thus, the following isentropic flow relations allow us to estimate the flow variables along the jet centerline in terms of the local pressure

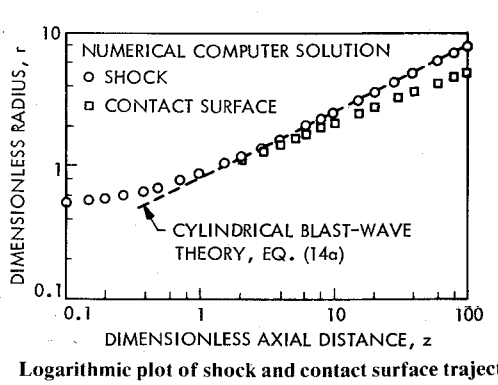

Fig. 9 Logarithmic plot of shock and contact surface trajectories.

$$\rho/\rho_1 = (p/p_1)^{1/\gamma}$$

$$h/h_1 = (p/p_1)^{(\gamma-1)/\gamma}$$

$$c/c_1 = (p/p_1)^{(\gamma-1)/2\gamma}$$

$$u_1^2 + 2(h_1 - h) \tag{15}$$

where the subscript refers to conditions in the hot plasma immediately behind the LSD wave as given by Eqs. (3). If we use the blast-wave prediction (14c) for the pressure, we obtain the following estimates

$$\rho = 0.361z^{-1/\gamma}$$

$$h = 1.07z^{-(\gamma-1)/\gamma}$$

$$c = 0.464z^{-(\gamma-1)/2\gamma}$$

$$u = 1.81[1 - 0.657z^{-(\gamma-1)/\gamma}]^{1/2} \tag{16}$$

The axial mass flow rate is roughly uniform across the jet up to the contact surface r_c. Thus, we can estimate the latter by using the global continuity equation

$$\rho u r_c^2 = (\rho u r_c^2)_1$$

to obtain

$$r_c = 0.168z^{1/2\gamma}[1 - 0.657z^{-(\gamma-1)/\gamma}]^{-1/4} \tag{17}$$

These simple equations agree within 10% or better with the numerical solution in the asymptotic region $z \gg 1$.

Acknowledgment

The research reported here was supported by the Defense Advanced Research Projects Agency.

References

[1] Hall, R. B., Maher, W. E., and Wei, P. S. P., "An Investigation of Laser-Supported Detonation Waves," Air Force Weapons Laboratory, Kirtland AFB, N. Mex., AFWL-TR-73-28, 1973.

[2] Raizer, Y. P., "Heating of a Gas by a Powerful Light Pulse," *Soviet Physics JETP*, Vol. 21, Nov. 1965, pp. 1009-1017.

[3] Buckley, F. I. Jr., "Mach Dick Location in Jets in Co-Flowing Airstreams," *AIAA Journal*, Vol. 13, Jan. 1975, pp. 105-106.

[4] Love, E. S., Grigsby, C. E., Lee, L. P., and Woodling, M. J., "Experimental and Theoretical Studies of Axisymmetric Free Jets," NASA TR-R-6, 1959.

[5] Hayes, W. D. and Probstein, R. F., *Hypersonic Flow Theory*, Academic Press, New York, 1959.

[6] Thomas, P. D., Vinokur, M., Bastianon, R., and Conti, R. J., "Numerical Solution for Three-Dimensional Inviscid Supersonic Flow," *AIAA Journal*, Vol. 10, July 1972, pp. 887-894.

[7] MacCormack, R. W., "The Effect of Viscosity in Hypervelocity Impact Cratering," AIAA Paper 69-354, Cincinnati, Ohio, 1969.

[8] Howe, J. T., "Lateral Expansion of a Laser-Supported Detonation Wave in a Gas," *AIAA Journal*, Vol. 10, Dec. 1972, pp. 1710-1711.

[9] "Equations, Tables, and Charts for Compressible Flow," Ames Aeronautical Laboratory, Moffett Field, Calif., Rept. 1135, 1953.

[10] Sedov, L. I., *Similarity and Dimensional Methods of Mechanics*, Academic Press, New York, 1959.

[11] Pirri, A. N., "Theory for Momentum Transfer to a Surface with a High Power Laser," *Physics of Fluids*, Vol. 16, Sept. 1973, pp. 1435-1440.

[12] O'Neil, R. W., et al., "High Energy Pulsed CO_2 Laser-Target Interaction in Air," Lincoln Laboratory, Massachusetts Institute of Technology, Lexington, Mass., LTP-17, Sept. 1972.

[13] Nielsen, P. E., "Momentum Transfer to Solid Targets in the Presence of Laser-Supported Detonation Waves," *Laser Digest*, Air Force Weapons Laboratory, Kirtland AFB, N. Mex., AFWL-TR-73-273, Dec. 1973, pp. 102-110.

[14] Kentzer, C. P., "Discretization of Boundary Conditions on Moving Discontinuities," *Proceedings of the Second International Conference on Numerical Methods in Fluid Dynamics*, Springer-Verlag, New York, 1971, pp. 108-113.